Potential Energy Curves and Lifetimes of Low-Lying Excited Electronic States of CSe Studied by Configuration Interaction Method

ARTICLE *in* THE JOURNAL OF PHYSICAL CHEMISTRY A · MARCH 2014

Impact Factor: 2.69 · DOI: 10.1021/jp411480s · Source: PubMed

5 AUTHORS, INCLUDING:

Rui Li
Jilin University
14 PUBLICATIONS **32** CITATIONS
SEE PROFILE

Mingxing Jin
Jilin University
91 PUBLICATIONS **383** CITATIONS
SEE PROFILE

Bing Yan
Jilin University
47 PUBLICATIONS **63** CITATIONS
SEE PROFILE

THE JOURNAL OF PHYSICAL CHEMISTRY A

Article

pubs.acs.org/JPCA

Potential Energy Curves and Lifetimes of Low-Lying Excited Electronic States of CSe Studied by Configuration Interaction Method

Rui Li,[†,‡] Erping Sun,[†] Mingxing Jin,[†] Haifeng Xu,[†,*] and Bing Yan*[,†]

[†]Institute of Atomic and Molecular Physics, Jilin University, Changchun 130012, China

[‡]Department of Physics, College of science, Qiqihar University, Qiqihar 161006, China

Supporting Information

ABSTRACT: In this work, we performed a high level ab initio study on the low-lying electronic states of CSe, utilizing MRCI+Q (the internally contracted multireference configuration interaction, and Davidson's correction) method with scalar relativistic and spin−orbit coupling effects taken into account. The potential energy curves of 18 Λ−S states associated with the lowest dissociation limit of CSe molecule, as well as those of 50 Ω states generated from the Λ−S states were computed. The spectroscopic parameters of bound states were evaluated, which agree well with existing theoretical and experimental results. With the aid of calculated spin−orbit matrix elements and the Λ−S compositional variation of the Ω states, the spin−orbit perturbations of low-lying states to the $A^1\Pi$ and $a^3\Pi$ states are analyzed. Finally, the transition dipole moments of $A^1\Pi$, $A'^1\Sigma^+$, $a^3\Pi_{0+}$, and $a^3\Pi_1$ to the ground $X^1\Sigma^+$ state as well as the lifetimes of the four excited states were evaluated.

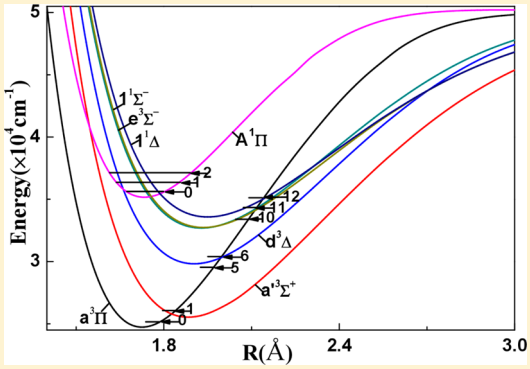

INTRODUCTION

Research interest in molecular CSe arises from its potential importance in the development of a mid-infrared CO chemical laser.[1−3] As one of the candidates in producing a CO chemical laser through the O + CSe → CO* + Se reaction, the electronic states of CSe have been intensively studied. The detailed information on the electronic states and spectroscopic parameters of CSe is very helpful for understanding the branching processes in the reaction mixture. Pioneering work on the ultraviolet band spectrum of CSe was carried out by Barrow in 1939.[4] Since then, several spectroscopic studies have been performed on the spin-allowed $A^1\Pi-X^1\Sigma^+$ transition and the spin-forbidden $a^3\Pi-X^1\Sigma^+$ transition. The $A^1\Pi-X^1\Sigma^+$ emission band system of CSe, consisting of seven bands, was observed between 2781 and 2948 Å by Laird et al.[5] The spectroscopic parameters of the $A^1\Pi$ and $X^1\Sigma^+$ states were derived from the rotational analysis of the seven bands, and the analysis result indicated that the $A^1\Pi$ state was heavily perturbed by interaction with other uncharacterized low-lying electronic states. Early study by Howell[6] indicated that the emission bands for the $a^3\Pi-X^1\Sigma^+$ transition of CSe are similar to the Cameron bands ($a^3\Pi-X^1\Sigma^+$ transition) of CO. Later, the vibrational[7] and rotational[8] resolved emission bands for the $a^3\Pi-X^1\Sigma^+$ transition were observed. The spin−orbit coupling (SOC) constant of the $a^3\Pi$ state[7] and isotopic shifts[8] of $^{12}C^{80}Se$ and $^{12}C^{78}Se$ were obtained from the emission spectra. Along with experimental investigations, several theoretical works[9−12] have been carried out to investigate the electronic ground state ($X^1\Sigma^+$) of CSe, using a number of ab initio computational methods. The geometric structure and the spectroscopic parameters of the $X^1\Sigma^+$ state were obtained. For the electronic excited states, to the best of our knowledge, there are no theoretical studies reported in the literature.

Despite various experimental and theoretical studies that have been carried out during the past several decades, our knowledge of the low-lying excited states of CSe is still lacking. The available experimental and theoretical studies are focused on the ground singlet $X^1\Sigma^+$ state, the lowest triplet $a^3\Pi$ state, and the first excited singlet $A^1\Pi$ state. The information about other excited electronic states is still missing. As indicated in previous studies of the isovalent molecules CS[13] and CO,[14] there exists a high density of excited states leading to strong state perturbations, making it a challenge to calculate the potential curves (PECs). In particular, the spin−orbit interaction plays a significant role in the spectroscopy and dynamics of the electronic states. This is especially important in CSe, because of the large spin−orbit effects in the heavy selenium atom.

In this work, we carried out a high level ab initio study on the low-lying electronic states of CSe. The PECs of the electronic states were calculated using the configuration interaction method including spin−orbit coupling (SOC) effects. On the

Received: November 22, 2013
Revised: March 21, 2014
Published: March 24, 2014

   dx.doi.org/10.1021/jp411480s | J. Phys. Chem. A 2014, 118, 2629−2637

basis of the calculated PECs, the spectroscopic constants of the bound states were obtained and compared with previous results. The transition dipole moments of the spin-allowed $A^1\Pi-X^1\Sigma^+$ and $A'^1\Sigma^+-X^1\Sigma^+$ transition, and the spin-forbidden transition of $a^3\Pi_i-X^1\Sigma^+$ were calculated. Finally, the radiative lifetimes of the low-lying vibrational states of the $A^1\Pi$, $A'^1\Sigma^+$, and $a^3\Pi_i$ were obtained.

METHODS AND COMPUTATIONAL DETAILS

In the present work, the ab initio calculations were carried out by employing the Molpro2010[15] program designed by Werner et al. The electronic calculations were done in the C_{2v} subgroup of the $C_{\infty v}$ point group, where the correlating relationships of the irreducible representations for the two groups are $\Sigma^+ = A_1$, $\Pi = B_1 + B_2$, $\Delta = A_1 + A_2$, and $\Sigma^- = A_2$. In all the calculations, we used the entirely uncontracted aug-cc-pwCV5Z basis set to describe the C[16] and Se[17] atoms. At a series of given internuclear distances between 1.2 and 3.7 Å, the 18 lowest Λ−S states for CSe were calculated using the state-averaged complete active space self-consistent field (CASSCF)[18,19] approach utilizing the Hartree−Fock molecular orbitals (MOs) as the starting orbitals. In the CASSCF calculations, the active space included eight MOs correlating to the C 2s2p and Se 4s4p valence orbitals. Subsequently, by utilizing the CASSCF energies as reference values, the energies of the 18 Λ−S states were computed with the internally contracted multireference configuration interaction approach (MRCI) with Davison size-extensivity correction (+Q).[20−22] For MRCI+Q calculations, the $2s^22p^2$ electrons of C and the $4s^24p^43d^{10}$ electrons of Se were correlated, whereas the remaining inner electrons were frozen and not correlated.

In the above calculations, the scalar relativistic effect was taken into consideration through the second-order Douglas−Kroll[23] and Hess[24] one-electron integrals. The SOC effect was treated by the state interaction method employing the full Breit−Pauli Hamilton (H_{BP}) operator.[25] The spin−orbit part of the H_{BP} operator is defined as

$$\hat{H}^{so} = \frac{e^2}{2m_e^2c^2}\sum_i\left[\sum_K \frac{Z_K}{r_{iK}^3}[\vec{r}_{iK}\times\vec{p}_i]\cdot\vec{s}_i - \sum_{j\neq i}\frac{1}{r_{ij}^3}[\vec{r}_{ij}\times\vec{p}_i]\cdot[\vec{s}_i + 2\vec{s}_j]\right] \quad (1)$$

where e is the electronic charge, m_e is the mass of the electron, c is the velocity of light, Z_K is the nuclear charge number of nucleus K, r_{ij} denotes the distance between electrons i and j, and

$$\vec{r}_{iK} = \vec{r}_i - \vec{R}_K$$

is the location of i with respect to the nucleus K. In the SOC calculations, the spin−orbit eigenstates were evaluated by diagonalizing $\hat{H}^{el} + \hat{H}^{so}$ matrix in the basis of the Λ−S wave functions. Additionally, the diagonal $\hat{H}^{el}$ matrix elements were acquired from MRCI+Q computations, and the $\hat{H}^{so}$ matrix elements were acquired from MRCI wave functions. The PECs were constructed by linking the energy points of electronic states considering the avoided crossing phenomenon between two states with the same Ω symmetry.

On the basis of fitted PECs of the bound and quasibound Λ−S and Ω electronic states, the corresponding vibrational energy levels, vibrational wave functions, Franck−Condon factors (FCFs), and spectroscopic parameters were obtained from the numerical solution of the one-dimensional nuclear Schrödinger equations employing LeRoy's LEVEL procedure.[26]

RESULTS AND DISCUSSION

A. PECs and Spectroscopic Properties of Λ−S States of CSe. The 18 Λ−S states correlated to the lowest dissociation limit ($C(^3P) + Se(^3P)$) of CSe were computed by the MRCI+Q approach utilizing the entirely uncontracted aug-cc-pwCV5Z basis set. The calculated PECs for all the 18 Λ−S states are presented in Figure 1. For visual clarity, the

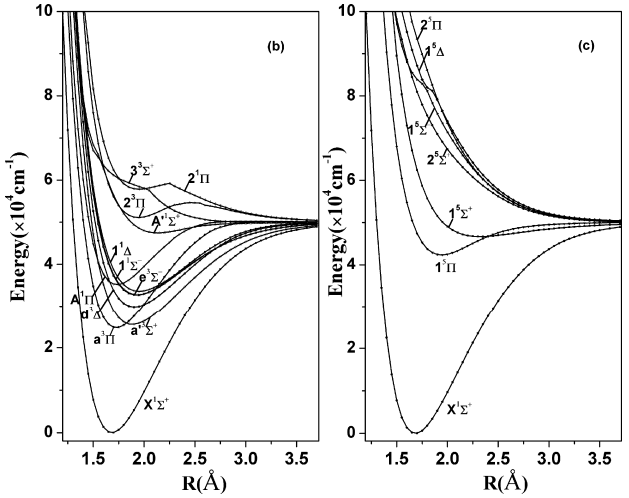

Figure 1. Calculated MRCI+Q potential energy curves of the low-lying Λ−S electronic states with (a) singlet and triplet and (b) quintet spin multiplicities. In each figure, the PEC of the ground state $X^1\Sigma^+$ is given for comparison.

singlet/triplet and the quintet Λ−S states are separately displayed in Figure 1a,b, along with the PEC of the ground state $X^1\Sigma^+$ in each figure for comparison. As shown in Figure 1a, except for four high-lying excited states, $A'^1\Sigma^+$, $2^3\Pi$, $2^1\Pi$, and $3^3\Sigma^+$, the other singlet/triplet electronic states are typical bound states with deep potential wells in the PECs. The $A'^1\Sigma^+$ state is weakly bound, and the two Π states ($2^3\Pi$ and $2^1\Pi$) are also weakly bound around R = 1.95 Å but change to be repulsive at larger internuclear distance, whereas the $3^3\Sigma^+$ state is a repulsive state. For quintet states, only the $1^5\Pi$ and $1^5\Sigma^+$ states are weakly bound; all the other quintet Λ−S states are repulsive (Figure 1b). The spectroscopic parameters of all the bound and quasibound Λ−S states were obtained and the results are listed in Table 1, including adiabatic transition energies T_e, harmonic vibrational frequencies ω_e, anharmonic terms $\omega_e x_e$, rotational constants B_e, and equilibrium distance R_e. For the ground $X^1\Sigma^+$ state, $a^3\Pi$, and $A^1\Pi$ states, our calculated spectroscopic constants agree well with previous experimental and theoretical results[5,7−12,27] (Table 1). The other states have been neither experimentally observed nor theoretically investigated in the literature.

As listed in Table 1, the equilibrium bond length of the $a^3\Pi$ state is similar as that of the $A^1\Pi$ state, which is less than 0.05 Å larger than that of the ground state, but evidently smaller than that of the $a'^3\Sigma^+$, $d^3\Delta$, $e^3\Sigma^-$, $1^1\Delta$. or $1^1\Sigma^-$ state. This may originate from the different electronic configuration compositions of these states. Table 2 shows the dominant electronic

dx.doi.org/10.1021/jp411480s | J. Phys. Chem. A 2014, 118, 2629−2637

Table 1. Computed and Experimental Spectroscopic Parameters of CSe[a]

state		T_e (cm^{-1})	ω_e (cm^{-1})	$\omega_e x_e$ (cm^{-1})	B_e (cm^{-1})	R_e (Å)
$X^1\Sigma^+$	this work	0	1028.36	4.7798	0.5700	1.6837
	expt	0	1035.9[b]/1035.9[c]	4.88[b]/4.87[c]	0.58[b]/0.574(5)[c]/0.5750[d]	1.669[b]/1.68[c]/1.676[d]
	calc	0	1038.8[e]/1012.7[f]/1035[g]/1037.55[h]	4.72[f]/4.8843[h]	0.552[f]/0.5711[h]	1.6776[e]/1.6925[f]/1.676[g]/1.6819[h]
$a^3\Pi$	this work	24733	899.94	5.7457	0.5428	1.7252
	expt	24317.4[c]/24381[i]	910(5)[c]/909[i]	8[c]/7[i]	0.544(5)[c]/0.5458[i]	1.72[c]/1.722[i]
$a'^3\Sigma^+$	this work	25535	682.54	3.6762	0.4556	1.8834
$d^3\Delta$	this work	29821	658.89	3.7664	0.4459	1.9037
$e^3\Sigma^-$	this work	32694	620.41	3.8141	0.4346	1.9282
$A^1\Pi$	this work	35168	831.68	8.0802	0.5380	1.7330
	expt	35134.6[b]/35136.414[d]	840[b]		0.50[b]	1.80[b]
$1^1\Sigma^-$	this work	32737	611.29	4.1162	0.4313	1.9356
$1^1\Delta$	this work	33583	589.28	4.0399	0.4249	1.9500
$1^5\Pi$	this work	42353	598.49	9.6041	0.4282	1.9425
$A'^1\Sigma^+$	this work	47473	413.91	16.9807	0.3547	2.1351
$2^3\Pi$	this work	51102	664.68	25.3797	0.4280	1.9428
$1^5\Sigma^+$	this work	46693	284.76	6.2192	0.2997	2.3211
$2^1\Pi$	this work	57844	496.10	17.7063	0.4258	1.9491

[a]For the experimental values, the uncertainty of the measurement is given in parentheses. [b]Reference 5. [c]Reference 7. [d]Reference 27. [e]Reference 9. [f]Reference 10. [g]Reference 11. [h]Reference12. [i]Reference 8.

Table 2. Dominant Electronic Configuration of Low-Lying Electronic States of CSe for R = 1.7 Å and R = 2.25 Å[a]

state	R = 1.7 Å	R = 2.25 Å
$X^1\Sigma^+$	$9\sigma^2 10\sigma^2 4\pi^4 11\sigma^2 5\pi^0$(87%)	$9\sigma^2 10\sigma^2 4\pi^4 11\sigma^2 5\pi^0$ (46%)
		$9\sigma^2 10\sigma^2 4\pi^3 11\sigma^2 5\pi^1$(39%)
$a^3\Pi$	$9\sigma^2 10\sigma^2 4\pi^4 11\sigma^1 5\pi^1$(83%)	$9\sigma^2 10\sigma^2 4\pi^4 11\sigma^1 5\pi^1$(56%)
		$9\sigma^2 10\sigma^2 4\pi^3 11\sigma^1 5\pi^2$(29%)
$a'^3\Sigma^+$	$9\sigma^2 10\sigma^2 4\pi^3 11\sigma^2 5\pi^1$(94%)	$9\sigma^2 10\sigma^2 4\pi^3 11\sigma^2 5\pi^1$(83%)
$A^1\Pi$	$9\sigma^2 10\sigma^2 4\pi^4 11\sigma^1 5\pi^1$(85%)	$9\sigma^2 10\sigma^2 4\pi^4 11\sigma^1 5\pi^1$(56%)
		$9\sigma^2 10\sigma^2 4\pi^3 11\sigma^1 3\pi^2$(30%)
$d^3\Delta$	$9\sigma^2 10\sigma^2 4\pi^3 11\sigma^2 5\pi^1$(93%)	$9\sigma^2 10\sigma^2 4\pi^3 11\sigma^2 5\pi^1$(89%)
$e^3\Sigma^-$	$9\sigma^2 10\sigma^2 4\pi^3 11\sigma^2 5\pi^1$(93%)	$9\sigma^2 10\sigma^2 4\pi^3 11\sigma^2 5\pi^1$(89%)
$1^1\Sigma^-$	$9\sigma^2 10\sigma^2 4\pi^3 11\sigma^2 5\pi^1$(93%)	$9\sigma^2 10\sigma^2 4\pi^3 11\sigma^2 5\pi^1$(87%)
$1^1\Delta$	$9\sigma^2 10\sigma^2 4\pi^3 11\sigma^2 5\pi^1$(91%)	$9\sigma^2 10\sigma^2 4\pi^3 11\sigma^2 5\pi^1$(86%)

[a]The percentage is given by the square of the CI coefficient in the CASSCF wave function.

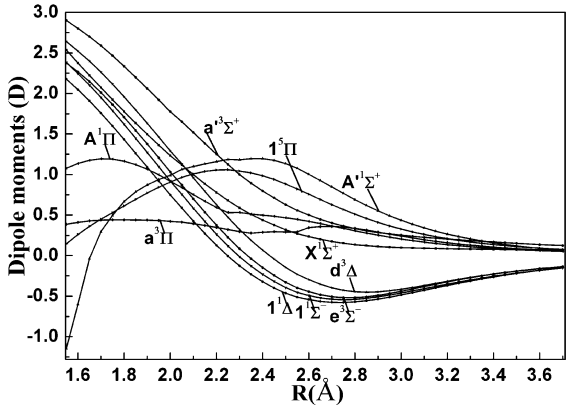

Figure 2. Evolution of dipole moments for some low-lying Λ−S electronic states along the internuclear distance.

configuration for the ground state $X^1\Sigma^+$ and the seven lowest excited states at R = 1.7 and 2.25 Å. The dominant electron configuration of the ground state $X^1\Sigma^+$ is $9\sigma^2 10\sigma^2 4\pi^4 11\sigma^2 5\pi^0$ at R = 1.7 Å, whereas that of the $a^3\Pi$ and $A^1\Pi$ states is $9\sigma^2 10\sigma^2 4\pi^4 11\sigma^1 5\pi^1$, corresponding to promotion of an electron from the 11σ MO to the vacant 5π MO. For the $a'^3\Sigma^+$, $d^3\Delta$, $e^3\Sigma^-$, $1^1\Delta$, and $1^1\Sigma^-$ states, the dominant electron configuration is $9\sigma^2 10\sigma^2 4\pi^3 11\sigma^2 5\pi^1$ at R = 1.7 Å, corresponding to promotion of an electron from the 4π MO to the vacant 5π MO. In contrast to the 4π MO, the 11σ MO is somewhat more nonbonding; thus the equilibrium bond lengths of the $a^3\Pi$ and $A^1\Pi$ states are smaller than those of the $a'^3\Sigma^+$, $d^3\Delta$, $e^3\Sigma^-$, $1^1\Delta$, and $1^1\Sigma^-$ states.

The dipole moments of the Λ−S states were calculated using MRCI wave functions. Dipole moment curves for some low-lying Λ−S states are plotted in Figure 2. At the equilibrium distance R = 1.6837 Å, the dipole moment of the ground state $X^1\Sigma^+$ is 2.13 D, which agrees well with the previous theoretical result of 2.14 D.[10] The positive dipole moment of the ground state indicates the $C^{\delta-}Se^{\delta+}$ polarity for the molecule. As shown in Figure 2, the dipole moments of all states are close to zero as $R \rightarrow \infty$, indicating the dissociation products are neutral atoms.

B. Analysis of Perturbations in $a^3\Pi$ and $A^1\Pi$ States. As shown in Figure 1, there is a large state density of CSe molecule in the investigated energy region, which leads to unavoidable interaction among these electronic states. Here, we focus on the perturbations in the $A^1\Pi$ and $a^3\Pi$ states arising from the spin−orbit interaction with other interacting states. Figure 3 presents an expanded view of the PECs of the states that may interact with the $A^1\Pi$ and $a^3\Pi$ states, together with the vibrational levels for the $A^1\Pi$ and $a^3\Pi$ states near the crossing points. As shown in Figure 3, both the $A^1\Pi$ and $a^3\Pi$ states cross with $1^1\Sigma^-$, $1^1\Delta$, $a'^3\Sigma^+$, $d^3\Delta$, and $e^3\Sigma^-$ states at internuclear distances between 1.55 and 2.15 Å. Considering the SOC effect, avoided crossings will occur at the crossing point of these states with other states of the same Ω value, which will make the PECs rather irregular. Hence, the position, shape and intensity of the spectrum for the corresponding states will be affected by the SOC effect. The $a^3\Pi$ state crosses with the $a'^3\Sigma^+$, $d^3\Delta$, $e^3\Sigma^-$, $1^1\Sigma^-$, and $1^1\Delta$ states at R = 1.83, 2.00, 2.12, 2.12, 2.14 Å, near v_a' = 1, 6, 11, 11, and 12 of the $a^3\Pi$ state, respectively. Because all the crossing

dx.doi.org/10.1021/jp411480s | J. Phys. Chem. A 2014, 118, 2629−2637

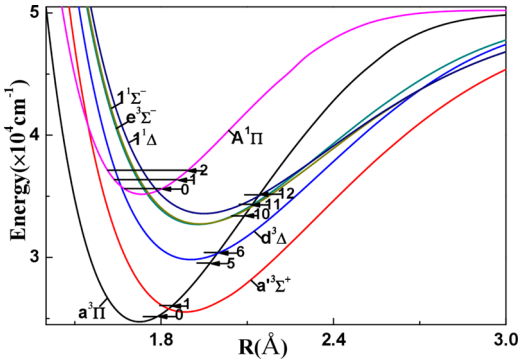

Figure 3. Expanded view of the crossing region of the potential energy curves for the electronic states $a^3\Pi$ and $A^1\Pi$ together with identity of vibrational levels for the two states around the crossing point.

points are located at $v_a' > 0$, the $v_a' = 0$ vibrational state is expected to be relatively unperturbed by interactions with other electronic states. This is one possible reason that the 0−0 band of the $a^3\Pi-X^1\Sigma^+$ band system could be easily observed in previous experiments.[7,8] The crossings between $A^1\Pi$ and the singlet states, $1^1\Delta$, $1^1\Sigma^-$ lie in the bottom of potential well of $A^1\Pi$ state. The selection rules that define what states may be coupled by the spin−orbit interaction for linear molecules ($\Delta\Omega = 0$; $\Delta\Lambda = 0, \pm1$; $\Delta\Sigma = 0, \mp1$; and $|S' - S| \leq 1 \leq S' + S$) imply that there can be no spin−orbit interactions between the $1^1\Delta$, $1^1\Sigma^+$, and $A^1\Pi$ states. The crossing positions between $A^1\Pi$ and the triplet states $a'^3\Sigma^+$, $d^3\Delta$, and $e^3\Sigma^-$ are located at internuclear distances R = 1.54, 1.66, and 1.76 Å, respectively. Except for the crossing point with $a'^3\Sigma^+$ (at R = 1.54 Å), the other two crossing points are located near the two lowest vibrational levels ($v_A' = 0$ and 1) of the $A^1\Pi$ state. Thus, perturbations caused by interactions with $d^3\Delta$ and $e^3\Sigma^-$ may affect the $v_A' = 0$ and 1 levels of the $A^1\Pi$ state.

To further examine the perturbations in $A^1\Pi$ and $a^3\Pi$, we computed the spin−orbit matrix elements between interacting electronic states. Panels a and b of Figure 4 display the variation of the absolute values for the spin−orbit matrix elements containing the $A^1\Pi$ and $a^3\Pi$ states with the internuclear distance. The definitions of the schematic terms for spin−orbit

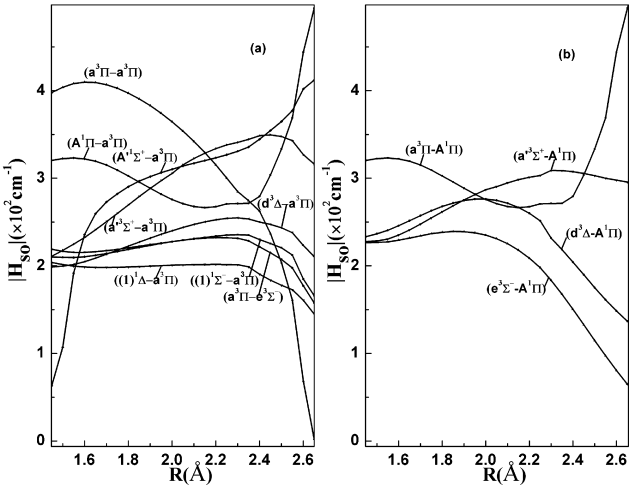

Figure 4. Absolute values of nonvanishing spin−orbit matrix elements containing (a) $a^3\Pi$ and (b) $A^1\Pi$ state as a function of the internuclear distance of the molecule CSe.

matrix elements used in Figure 4 are provided in Table 3. The spin−orbit matrix elements display similar behaviors for the

Table 3. Spin−Orbit Matrix Elements between Two Interacting Electronic States in the Curves Crossing Region[a]

$i\langle a^3\Pi_x, m_s=1 \vert L_zS_z \vert a^3\Pi_y, m_s=1\rangle = (a^3\Pi - a^3\Pi)$
$\langle (1)^3\Sigma^+, m_s=0 \vert L_yS_y \vert a^3\Pi_x, m_s=1\rangle = ((1)^3\Sigma^+ - a^3\Pi)$
$\langle (1)^3\Delta_x, m_s=0 \vert L_yS_y \vert a^3\Pi_x, m_s=1\rangle = ((1)^3\Delta - a^3\Pi)$
$\langle (1)^1\Delta_x, m_s=0 \vert L_yS_y \vert a^3\Pi_x, m_s=1\rangle = ((1)^1\Delta - a^3\Pi)$
$i\langle (1)^1\Sigma^-, m_s=0 \vert L_xS_x \vert a^3\Pi_x, m_s=1\rangle = ((1)^1\Sigma^- - a^3\Pi)$
$i\langle a^3\Pi_x, m_s=0 \vert L_xS_x \vert (1)^3\Sigma^-, m_s=1\rangle = (a^3\Pi - (1)^3\Sigma^-)$
$\langle A'^1\Sigma^+, m_s=0 \vert L_yS_y \vert a^3\Pi_x, m_s=1\rangle = (A'^1\Sigma^+ - a^3\Pi)$
$\langle A^1\Pi_x, m_s=0 \vert L_yS_y \vert a^3\Pi_y, m_s=0\rangle = (A^1\Pi - a^3\Pi)$
$\langle A^1\Pi_x, m_s=0 \vert L_yS_y \vert (1)^3\Sigma^+, m_s=1\rangle = (A^1\Pi - (1)^3\Sigma^+)$
$i\langle A^1\Pi_x, m_s=0 \vert L_xS_x \vert (1)^3\Sigma^-, m_s=1\rangle = (A^1\Pi - (1)^3\Sigma^-)$
$\langle {}^1\Pi_x, m_s=0 \vert L_xS_x \vert (1)^3\Delta_x, m_s=1\rangle = (A^1\Pi - (1)^3\Delta)$

[a]Between parentheses is the given schematic terms in Figure 4, the symbol i in front of angular bracket indicate the imaginary part of spin−orbit matrix elements.

coupling between the $a^3\Pi$ state and the $a'^3\Sigma^+$, $d^3\Delta$, $e^3\Sigma^-$, $1^1\Delta$, or $1^1\Sigma^-$ states, which first gradually increase as the C−Se bond length increases and then decrease rapidly at large internuclear distance. The evolution of spin−orbit matrix elements for the ($a^3\Pi-a^3\Pi$), ($a^3\Pi-A'^1\Sigma^+$), and ($A^1\Pi-a^3\Pi$) pairs, on the other hand, are evidently different. The spin−orbit interactions between that $a^3\Pi$ state and the $a'^3\Sigma^+$, $d^3\Delta$, $e^3\Sigma^-$, $1^1\Delta$, and $1^1\Sigma^-$ states are fairly similar at all internuclear separations because all of the latter states derive almost entirely from the same $9\sigma^2 10\sigma^2 4\pi^4 11\sigma^1 5\pi^1$ electronic configuration, and the contribution from this configuration is nearly unchanged between R = 1.7 Å and R = 2.25 Å. Due to the same leading electronic configurations of the $A^1\Pi$ state and the $a^3\Pi$ state ($9\sigma^2 10\sigma^2 4\pi^4 11\sigma^1 5\pi^1$ at R = 1.7 Å, $9\sigma^2 10\sigma^2 4\pi^4 11\sigma^1 5\pi^1$ and $9\sigma^2 10\sigma^2 4\pi^3 11\sigma^1 5\pi^2$ at R = 2.25 Å), the spin−orbit matrix element curves containing the $A^1\Pi$ state are similar to those containing the $a^3\Pi$ state, except that the maximum values of the elements are at somewhat different internuclear distances. At the crossing points, the values of spin−orbit integrals of $a^3\Pi-a'^3\Sigma^+$, $a^3\Pi-d^3\Delta$, $a^3\Pi-e^3\Sigma^-$, $a^3\Pi-1^1\Delta$, and $a^3\Pi-1^1\Sigma^-$ are 275.7, 240.4, 230.9, 201.5, and 232.6 cm^{-1}, respectively, and those of $A^1\Pi-a'^3\Sigma^+$, $A^1\Pi-d^3\Delta$, and $A^1\Pi-e^3\Sigma^-$ are 230.5, 241.8, and 237.0 cm^{-1}, respectively. The electronic spin−orbit interaction parameters of molecular CSe have not yet been obtained in experiment, whereas those parameters[28] of another carbon chalcogenide, CS, have been acquired from the ultraviolet (UV) spectrum. They were determined to be 78.5, 103.6, 74.3, 60.8, 102.3, and 73.2 cm^{-1} for $a^3\Pi-a'^3\Sigma^+$, $a^3\Pi-d^3\Delta$, $a^3\Pi-e^3\Sigma^-$, $A^1\Pi-a'^3\Sigma^+$, $A^1\Pi-d^3\Delta$, and $A^1\Pi-e^3\Sigma^-$, respectively. Because the atomic number of Se is larger than that of S, the spin−orbit interaction parameters of CSe are expected to be larger than those of CS. The absolute values of spin−orbit matrix elements containing $A^1\Pi$ and $a^3\Pi$ are distributed in the range of 201.5−275.7 cm^{-1}, which is high enough to perturb the corresponding vibrational wave functions of the two states.

C. PECs and Spectroscopic Properties of Ω States of CSe. The SOC effect causes the splitting of multiplet electronic states and mixing of Λ−S states with common Ω symmetry. Therefore, once the SOC effect is included in the calculations, the lowest dissociation limit of $Se(^3P) + C(^3P)$ splits into nine asymptotes, namely $C(^3P_0)-Se(^3P_2)$, $C(^3P_1)-Se(^3P_2)$, C-

dx.doi.org/10.1021/jp411480s | J. Phys. Chem. A 2014, 118, 2629−2637

($^3P_2$)−Se($^3P_2$), C($^3P_0$)−Se($^3P_1$), C($^3P_1$)−Se($^3P_1$), C($^3P_2$)−Se($^3P_1$), C($^3P_0$)−Se($^3P_0$), C($^3P_1$)−Se($^3P_0$), and C($^3P_2$)−Se($^3P_0$). The Ω-states deriving from these separated atom limits are provided in Table 4. The computed atomic energy level

Table 4. Relationships between Dissociation Limit and Correlating Ω States of CSe

		energy (cm^{-1})	
atomic state (C + Se)	Ω state	this work	expt[a]
$^3P_0$ + $^3P_2$	2,1,0^+	0	0
$^3P_1$ + $^3P_2$	3,2,2,1,1,1,0^+,0^-,0^-	13	13
$^3P_2$ + $^3P_2$	4,3,3,2,2,2,1,1,1,1,0^+,0^+,0^+,0^-,0^-	40	39
$^3P_0$ + $^3P_1$	1,0^-	1798	1989
$^3P_1$ + $^3P_1$	2,1,1,0^+,0^+,0^-	1811	2002
$^3P_2$ + $^3P_1$	3,2,2,1,1,1,0^+,0^-,0^-	1838	2028
$^3P_0$ + $^3P_0$	0^+	2697	2534
$^3P_1$ + $^3P_0$	1,0^-	2710	2547
$^3P_2$ + $^3P_0$	2,1,0^+	2737	2573

[a]Reference 29.

splitting is 13 cm^{-1} for $^3P_1$−$^3P_0$ of C, 40 cm^{-1} for $^3P_2$−$^3P_0$ of C, 1798 cm^{-1} for $^3P_0$−$^3P_1$ of Se, and 2697 cm^{-1} for $^3P_0$−$^3P_2$ of Se, respectively, which are in good agreement with the corresponding experimental values of 13, 39, 1989, and 2534 cm^{-1}.[29]

Altogether, there are a total of 50 Ω states of 4, 3, 2, 1, 0^+, and 0^- symmetry correlated to nine separated atom asymptotes. The PECs for all 50 Ω states have been computed, but we will not illustrate the repulsive high-lying states in this work. There are 25 low-lying bound Ω states located in excitation energy range of 0−47300 cm^{-1}. The PECs of the 25 Ω states are presented in Figure 5, including five Ω = 0^- states, five Ω = 0^+ states, eight Ω = 1 states, five Ω = 2 states, and two Ω = 3 states. For clarity, the PECs of 0^-, 0^+, 1, 2, and 3 states are displayed separately in Figure 5a−d, respectively.

Due to the SOC effect, the different Λ−S composition of Ω states varies gradually as a function of the internuclear distance. The compositions of the low-lying Ω states at several selected bond lengths near the avoided crossing points are listed in Table S3 (Supporting Information). The spectroscopic parameters of the 25 Ω states were numerically evaluated, and the corresponding results are given in Table 5. Because the ground state $X^1\Sigma^+$ is a singlet state, it does not undergo splitting due to the SOC effect. Inclusion of the spin−orbit interaction only lowers the electronic energy by about 38.81 cm^{-1} near the equilibrium internuclear distance. As illustrated in Table S3 (Supporting Information), the ground state $X0^+$ is composed of 99.7% $X^1\Sigma^+$ Λ−S state; thus the spectroscopic constants of the $X0^+$ state given in Table 5 are almost the same as those of the $X^1\Sigma^+$ state in Table 1. With the inclusion of the SOC effect, the different Λ−S electronic states may interact, and the mixing of electronic states with the same Ω symmetry could lead to avoided crossing in the PECs. Hence, the spectroscopic parameters for the majority of the Ω states in Table S3 (Supporting Information) are evidently different from those for the pure Λ−S electronic states in Table 1.

As mentioned in the above section, the $a^3\Pi$ state crosses with $a'^3\Sigma^+$, $d^3\Delta$, $e^3\Sigma^-$,$1^1\Delta$, and $1^1\Sigma^-$ states in the energy range 25500−35200 cm^{-1}, at R = 1.83−2.14 Å (Figure 3), and the SOC between the five states and $a^3\Pi$ all have nonvanishing spin−orbit interaction parameters (Figure 4a). According to the selection rules of the $\hat{H}^{so}$ operator, the avoided crossings only occur between electronic states with the same Ω symmetries. The $a^3\Pi$ state has four Ω components, namely 0^-, 0^+, 1, and 2, and the other nearby five Λ−S states ($a'^3\Sigma^+$, $d^3\Delta$, $e^3\Sigma^-$,$1^1\Delta$, and $1^1\Sigma^-$) split into two Ω = 0^-, one Ω = 0^+, three Ω = 1, two Ω = 2, and one Ω = 3 states; hence, there are

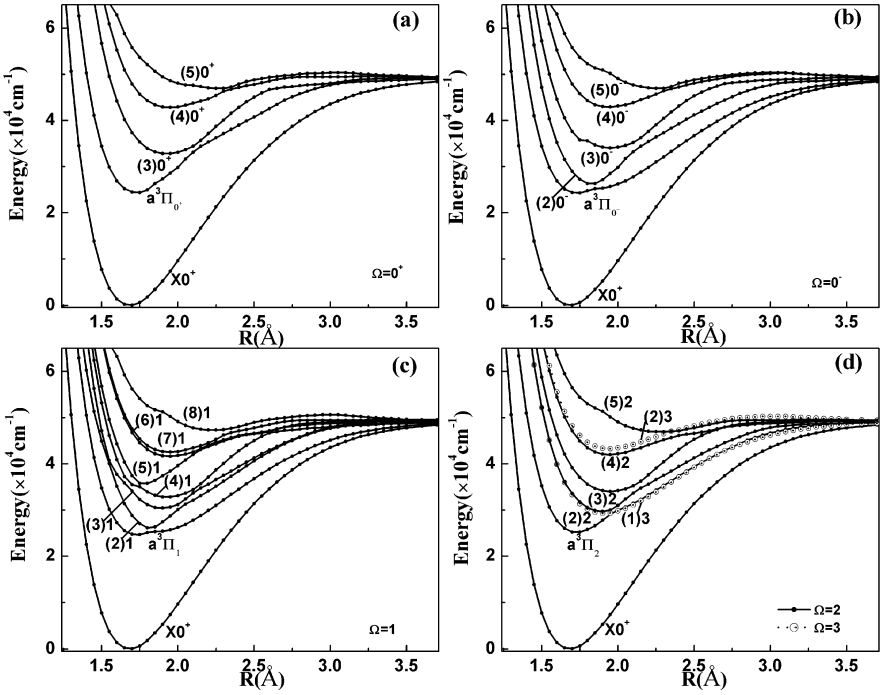

Figure 5. Potential energy curves with the spin−orbit coupling effect of the low-lying electronic states of CSe molecule for (a) Ω = 0^+, (b) Ω = 0^-, (c) Ω = 1, and (d) Ω = 2 and 3 states. In each figure, the PEC of the ground state $X0^+$ is displayed for comparison.

dx.doi.org/10.1021/jp411480s | J. Phys. Chem. A 2014, 118, 2629−2637

Table 5. Computed Spectroscopic Constants of Low-Lying Ω States of CSe

state		T_e (cm^{-1})	ω_e (cm^{-1})	$\omega_e x_e$ (cm^{-1})	B_e (cm^{-1})	R_e (Å)
$X0^+$	this work	0	1027.84	4.7863	0.5699	1.6838
	expt	0	1035.9[a]/1035.9[b]	4.88[a]/4.87[b]	0.58[a]/0.574(5)[b] /0.5750[c]	1.669[a]/1.68[b] /1.676[c]
	calc	0	1038.8[d]/1012.7[e] / 1035[f]/1037.55[g]	4.72[e]/4.8843[g]	0.552[e]/0.5711[g]	1.6776[d]/1.6925[e] /1.676[f]/1.6819[g]
$a^3\Pi_{0-}$	this work	24308	644.00	6.3647	0.5493	1.7288
$a^3\Pi_{0+}$	this work	24402	925.07	8.2888	0.5410	1.7242
	expt	24080.0[b]/24144(1)[h]	910(5)[b]/909[h]	8[b]/7[h]	0.544(5)[b]/0.5452(2)[h]	1.72[b]/1.722[h]
$a^3\Pi_1$	this work	24660	653.76	45.8724	0.5579	1.7281
	expt	24396.6[b]/24460(1)[h]			0.544(5)[b]/0.5474(2)	1.72[b]/1.722[h]
$a^3\Pi_2$	this work	25180	905.52	15.8461	0.5420	1.7265
(2)1	this work	26159	1149.05	30.7239	0.4953	1.8065
$(2)0^-$	this work	26216	1082.48	19.1208	0.4850	1.8241
(3)1	this work	30423	771.75	9.8622	0.4493	1.8950
(1)3	this work	29276	653.72	3.7914	0.4449	1.9059
(2)2	this work	29715	850.85	11.8276	0.4489	1.9018
(4)1	this work	32826	605.46	−1.2322	0.4354	1.9246
$(3)0^+$	this work	32826	643.18	−2.4781	0.4356	1.9246
$(3)0^-$	this work	34066	594.86	−1.9836	0.4263	1.9484
(5)1	this work	35584	1137.50	29.2910	0.5143	1.7702
(3)2	this work	34065	627.37	−2.0891	0.4265	1.9457
(2)3	this work	43295	585.26	9.7792	0.4287	1.9414
(4)2	this work	42031	620.09	14.1155	0.4277	1.9437
(6)1	this work	41648	640.79	13.6089	0.4272	1.9443
(7)1	this work	42517	621.04	10.8403	0.4279	1.9432
$(4)0^+$	this work	42821	604.56	10.8469	0.4274	1.9444
$(4)0^-$	this work	42896	602.00	10.1002	0.4290	1.9407
$(5)0^+$	this work	46902	491.45	15.7447	0.3122	2.2803
$(5)0^-$	this work	46890	552.55	19.2922	0.3155	2.2803
(8)1	this work	47259	507.39	16.0490	0.3263	2.2266
(5)2	this work	46913	382.40	4.3384	0.3113	2.2787

[a]Reference 5. [b]Reference 7. [c]Reference 27. [d]Reference 9. [e]Reference 10. [f]Reference 11. [g]Reference 12. [h]Reference 8.

eight avoided crossing points (two for Ω= 0^-, one for Ω = 0^+, three for Ω = 1, and two for Ω = 2 states) distributed in the region of R = 1.8−2.2 Å (Figure 5). As displayed in Table S3 (Supporting Information), around the avoided crossing points, the Λ−S compositions of the Ω-states vary rapidly, illustrating the obvious SOC effect on the states. For the $a^3\Pi_{0+}$ state, the avoided crossing point occurs at R = 2.15 Å, and the dominant Λ−S composition varies from 98.1% $^3\Pi$ at R = 1.95 Å to 62.2% $^3\Sigma^-$ at R = 2.15 Å. Because the avoided crossing point position occurs near the v = 11 vibrational level of $a^3\Pi_{0+}$, the v=0−10 vibrational levels of $a^3\Pi_{0+}$ are free from perturbations by the crossing states, and the emission spectrum of $a^3\Pi_{0+}$−$X^1\Sigma^+$ has been observed in experiment.[7,8] The deviation between our calculated values and the experimental values[8] is 258 cm^{-1}, 16.07 cm^{-1}, 1.2888 cm^{-1}, 0.0042 cm^{-1}, and 0.0022 Å, for T_e, ω_e, $\omega_e x_e$, B_e, and R_e, respectively. For the $a^3\Pi_1$ state, the avoided crossing point occurs at R = 1.85 Å, and the dominant Λ−S composition changes from 86.2% $^3\Pi$ at R = 1.80 Å to 85.8% $^3\Sigma^+$ at R = 1.85 Å. The avoided crossing point lies between the two lowest vibrational levels (v_a' = 0 and 1) of the $a^3\Pi_1$ state; hence, the $v_a' \geq 1$ vibrational levels of $a^3\Pi_1$ are strongly perturbed by the crossing state ($a'^3\Sigma^+$). Because only the v_a' = 0 vibrational level of $a^3\Pi_1$ is free from perturbations by other crossing states, the ω_e and $\omega_e x_e$ values of the $a^3\Pi_1$ state could not be experimentally determined and only the T_e, B_e, and R_e parameters of the v_a' = 0 level were obtained.[7,8] Our theoretical T_e, B_e, and R_e values of $a^3\Pi_1$ are 24660 cm^{-1}, 0.5579 cm^{-1}, and 1.7281 Å, respectively, agree well with latest experimental results[8] of 24460 cm^{-1}, 0.5474 cm^{-1}, and 1.722 Å.

As to the singlet $A^1\Pi$ state, it has only one component of Ω = 1; therefore, there are three avoided crossing points between $a'^3\Sigma^+$, $d^3\Delta$, $e^3\Sigma^-$, and $A^1\Pi$ located in the region of R = 1.5−1.8 Å (Figure 5). The avoided crossing points break up the PECs of the $A^1\Pi$ state into four pieces, i.e., (2)1 at $R \leq$ 1.55 Å, (3)1 at R = 1.6, 1.65 Å, (4)1 at R = 1.7 Å, (5)1 at $R \geq$ 1.75 Å (see the Λ−S composition in Table S3, Supporting Information). The dominant Λ−S state composition of the (2)1 state changes from $^1\Pi$(73.7%) at R = 1.55 Å to $^3\Sigma^+$ (97.3%) at R = 1.6 Å, that of the (3)1 state changes from 95.8% $^1\Pi$ at R = 1.6 Å to 86.9% $^3\Delta$ at R = 1.70 Å, that of the (4)1 state changes from 83.3% $^1\Pi$ at R = 1.7 Å to 52.1% $^3\Sigma^-$ at R = 1.75 Å, and that of the (5)1 state changes from 51.1% $^1\Pi$ at R = 1.75 Å to 93.8% $^1\Pi$ at R = 1.80 Å. In the internuclear region of R = 1.5−1.8 Å, the vibrational wave functions of $A^1\Pi_1$ state are heavily perturbed by contributions of the wave functions of $a'^3\Sigma^+$, $d^3\Delta$, and $e^3\Sigma^-$. Because the transitions from the three triplet states to the ground singlet state $X^1\Sigma^+$ are spin-forbidden transitions, the admixtures of the three triplet states may reduce the transition probabilities and increase the radiative lifetime of the $A^1\Pi$ state.

D. Transition Properties Analysis and Lifetimes. The transition dipole moments (TDMs) of the spin-allowed $A^1\Pi$−$X^1\Sigma^+$ and $A'^1\Sigma^+$−$X^1\Sigma^+$ transitions, and four spin-forbidden transitions, $a^3\Pi_{0+}((2)0^+)$−$X0^+$, $e^3\Sigma_{0+}^-((3)0^+)$−$X0^+$, $a^3\Pi_1((1)1)$−$X0^+$, and $a'^3\Sigma^+((2)1)$−$X0^+$, were computed from the spin−orbit coupled wave functions. The evolution of each

dx.doi.org/10.1021/jp411480s | J. Phys. Chem. A 2014, 118, 2629−2637

TDM along the internuclear distance is displayed in Figure 6a,b for the spin-allowed transitions and spin-forbidden transitions,

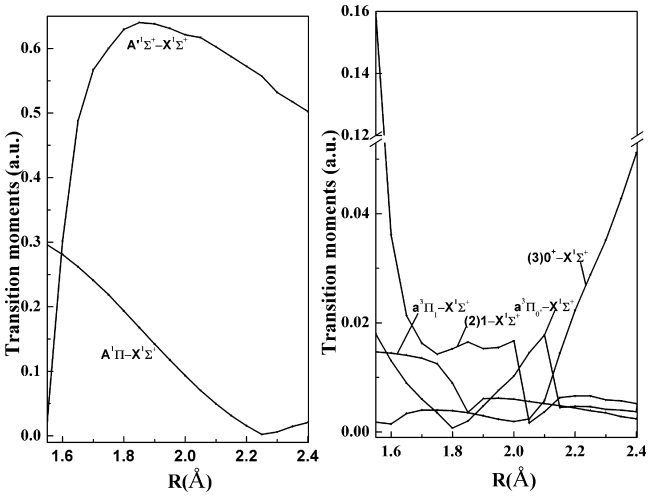

Figure 6. Transition dipole moments for (a) spin-allowed transitions $A^1\Pi-X^1\Sigma^+$ and $A'^1\Sigma^+-X^1\Sigma^+$, (b) spin-forbidden transitions, $a^3\Pi_{0+}((2)0^+)-X0^+$, $(3)0^+-X0^+$, $a^3\Pi_1((1)1)-X0^+$, and $(2)1-X0^+$ transitions as a function of internuclear distance of CSe molecule.

respectively. The TDMs of triplet-singlet transitions are at least 1 order of magnitude smaller than those of singlet−singlet transitions around the equilibrium distance of R = 1.6837 Å. In the Franck−Condon region, the TDM of the $A^1\Pi-X^1\Sigma^+$ transition is smaller than that of the $A'^1\Sigma^+-X^1\Sigma^+$ transition. Because the Λ−S compositions of $(2)0^+$ and $(1)1$ states exchange with those of $(3)0^+$ and $(2)1$ states near the their respective avoided crossing points, the transition properties of $(2)0^+$ and $(1)1$ states will be heavily perturbed by $(3)0^+$ and $(2)1$ states; hence, we give the transition dipole moments from all four states $(2)0^+$, $(3)0^+$, $(1)1$, and $(2)1$ to the ground state $X0^+$ in Figure 6b. It can be seen from the figure that the TDM of the $a^3\Pi_{0+}-X0^+$ decreases sharply at R = 2.15 Å, which could be caused by the $X^1\Sigma^+$ Λ−S compositional percentage of $(2)0^+$ varied from 0.31% at R = 2.05 Å to 0.02% at R = 2.15 Å. Similar to the TDM of the $a^3\Pi_{0+}-X0^+$, that of $a^3\Pi_1-X0^+$ also decreases evidently at R = 1.85 Å, which could be attributed to the $A^1\Pi$ Λ−S compositional percentage of $a^3\Pi_1$ that varied from 0.07% at R = 1.75 Å to 0.03% at R = 1.85 Å.

The Einstein coefficients $A_{v'v''}$, Franck−Condon Factors (FCFs), and transition energies $T_{v'v''}$ for different vibrational states, which determine the transition probabilities for the emission from excited states to the ground state, were calculated for $A^1\Pi-X^1\Sigma^+$, $A'^1\Sigma^+-X^1\Sigma^+$, $a^3\Pi_{0+}-X0^+$, and $a^3\Pi_1-X0^+$ transitions, and the results are listed in Tables 6−9, respectively. It can be seen from Tables 6−9 that the relative intensities of FCFs are overall in accord with those of Einstein coefficients. For $a^3\Pi_{0+}-X0^+$, $a^3\Pi_1-X0^+$, and $A^1\Pi-X^1\Sigma^+$ transitions, the (0,0) band is expected to the strongest vibronic transition, whereas for the $A'^1\Sigma^+-X^1\Sigma^+$ transition, the (0,16) band is predicted to be the most intense, due to the large equilibrium distance of $A'^1\Sigma^+$. The large equilibrium distance of $A'^1\Sigma^+$ also causes the largest Einstein coefficients, $A_{v'v''}$, to correspond to the v'' = 8−17 vibrational levels of $X^1\Sigma^+$ and the v' = 0−4 vibrational levels of $A'^1\Sigma^+$. Our calculated T_{00} of $a^3\Pi_{0+}-X0^+$, $a^3\Pi_1-X0^+$, and $A^1\Pi-X^1\Sigma^+$ transitions are 24327, 24563, and 35069 cm^{-1}, respectively, which agree well with the experimental values of 24091.3,[7] 24407.0,[7] and 35136.414 cm^{-1}.[27] For the $A'^1\Sigma^+-X^1\Sigma^+$ transition, the T_{00} is calculated to be 31994 cm^{-1}, but the experimental T_{00} is not yet known.

The radiative lifetime for a given vibrational level (v') of excited state is obtained from the inverse of the total Einstein

Table 6. Einstein Coefficients $A_{v'v''}$ ($\times 10^6$ s^{-1}), Franck−Condon Factors (FCFs), and Transition Energies $T_{v'v''}$ (cm^{-1}) for the $A^1\Pi-X^1\Sigma^+$ Transition of CSe Molecule

v''		v' = 0	v' = 1	v' = 2	v' = 3	v' = 4
0	$A_{v'v''}$	3.2561	1.2742	0.2581	0.0345	0.0035
	FCFs	0.6865	0.2562	0.0499	0.0066	0.0007
	$T_{v'v''}$	35069	35884	36683	37466	38233
1	$A_{v'v''}$	1.0945	1.1262	1.6313	0.6080	0.1323
	FCFs	0.2521	0.2469	0.3429	0.1270	0.0267
	$T_{v'v''}$	34050	34865	35664	36447	37214
2	$A_{v'v''}$	0.2079	1.3855	0.1683	1.3159	0.9140
	FCFs	0.0524	0.3318	0.0386	0.2991	0.1999
	$T_{v'v''}$	33040	33855	34654	35437	36204
3	$A_{v'v''}$	0.0286	0.4937	1.1369	0.0127	0.7842
	FCFs	0.0079	0.1293	0.2844	0.0031	0.1866
	$T_{v'v''}$	32040	32855	33654	34437	35205
4	$A_{v'v''}$	0.0031	0.1042	0.7247	0.6428	0.2305
	FCFs	0.0009	0.0299	0.1983	0.1737	0.0597
	$T_{v'v''}$	31050	31865	32664	33447	34215
5	$A_{v'v''}$	0.0003	0.0159	0.2255	0.7820	0.2305
	FCFs	0.0001	0.0050	0.0676	0.2311	0.0652
	$T_{v'v''}$	30070	30885	31684	32467	33234

Table 7. Einstein Coefficients $A_{v'v''}$ ($\times 10^6$ s^{-1}), Franck−Condon Factors (FCFs), and Transition Energies $T_{v'v''}$ (cm^{-1}) for the $A'^1\Sigma^+-X^1\Sigma^+$ Transition of CSe Molecule

v''		v' = 0	v' = 1	v' = 2	v' = 3	v' = 4
8	$A_{v'v''}$	0.1274	0.5841	1.2968	1.8393	1.9367
	FCFs	0.0030	0.0137	0.0305	0.0439	0.0449
	$T_{v'v''}$	39270	39642	39994	40325	40629
9	$A_{v'v''}$	0.2693	1.0259	1.8450	2.0391	1.5743
	FCFs	0.0068	0.0258	0.0467	0.0522	0.0392
	$T_{v'v''}$	38328	38699	39052	39383	39686
10	$A_{v'v''}$	0.5038	1.5523	2.1614	1.7072	0.7946
	FCFs	0.0136	0.0420	0.0588	0.0470	0.0212
	$T_{v'v''}$	37394	37766	38119	38450	38753
11	$A_{v'v''}$	0.8414	2.0256	2.0371	0.9650	0.1311
	FCFs	0.0245	0.0590	0.0596	0.0286	0.0038
	$T_{v'v''}$	36471	36843	37195	37526	37830
12	$A_{v'v''}$	1.2642	2.2689	1.4634	0.2500	0.0448
	FCFs	0.0398	0.0712	0.0462	0.0080	0.0014
	$T_{v'v''}$	35557	35928	36281	36612	36916
13	$A_{v'v''}$	1.7192	2.1529	0.6966	0.0022	0.4656
	FCFs	0.0585	0.0730	0.0237	0.0001	0.0155
	$T_{v'v''}$	34652	35024	35376	35707	36011
14	$A_{v'v''}$	2.1274	1.6820	0.1270	0.2909	0.8556
	FCFs	0.0782	0.0616	0.0047	0.0108	0.0307
	$T_{v'v''}$	33757	34129	34481	34812	35116
15	$A_{v'v''}$	2.4071	1.0147	0.0210	0.7533	0.7771
	FCFs	0.0959	0.0402	0.0008	0.0302	0.0301
	$T_{v'v''}$	32871	33243	33595	33926	34230
16	$A_{v'v''}$	2.4996	0.3972	0.3385	0.9291	0.3378
	FCFs	0.1080	0.0171	0.0146	0.0402	0.0142
	$T_{v'v''}$	31994	32366	32719	33050	33353
17	$A_{v'v''}$	2.3898	0.0444	0.7765	0.6707	0.0169
	FCFs	0.1121	0.0021	0.0362	0.0315	0.0008
	$T_{v'v''}$	31128	31499	31852	32183	32486

dx.doi.org/10.1021/jp411480s | J. Phys. Chem. A 2014, 118, 2629−2637

Table 8. Einstein Coefficients $A_{v'v''}$ ($\times 10^2$ s^{-1}), Franck–Condon Factors (FCFs), and Transition Energies $T_{v'v''}$ (cm^{-1}) for the $a^3\Pi_{0+}$–$X^1\Sigma^+$ Transition of CSe Molecule

v''		$v'=0$	$v'=1$	$v'=2$	$v'=3$	$v'=4$
0	$A_{v'v''}$	3.1263	1.1789	0.2173	0.0230	0.0036
	FCFs	0.7685	0.2043	0.0246	0.0023	0.0003
	$T_{v'v''}$	24327	25251	26206	27074	27892
1	$A_{v'v''}$	0.7359	2.2669	2.1531	0.5675	0.1301
	FCFs	0.2057	0.4446	0.2749	0.0629	0.0106
	$T_{v'v''}$	23309	24233	25187	26056	26874
2	$A_{v'v''}$	0.0771	1.3562	1.7815	2.1806	1.2145
	FCFs	0.0246	0.3021	0.2572	0.2721	0.1112
	$T_{v'v''}$	22300	23224	24179	25047	25865
3	$A_{v'v''}$	0.0034	0.1846	2.1589	0.7244	2.7691
	FCFs	0.0013	0.0469	0.3538	0.1021	0.2854
	$T_{v'v''}$	21300	22224	23180	24047	24866
4	$A_{v'v''}$	0	0.0067	0.4326	2.3301	0.0748
	FCFs	0	0.0020	0.0808	0.3727	0.0087
	$T_{v'v''}$	20311	21235	22190	23058	23876
5	$A_{v'v''}$	0	0	0.0344	0.8371	2.3051
	FCFs	0	0	0.0074	0.1525	0.3043
	$T_{v'v''}$	19331	20255	21210	22078	22896

Table 9. Einstein Coefficients $A_{v'v''}$ ($\times 10^2$ s^{-1}), Franck–Condon Factors (FCFs), and Transition Energies $T_{v'v''}$ (cm^{-1}) for the $a^3\Pi_1$–$X^1\Sigma^+$ Transition of CSe Molecule

v''		$v'=0$	$v'=1$	$v'=2$	$v'=3$	$v'=4$
0	$A_{v'v''}$	26.2555	4.5846	3.3262	0.9843	0.3051
	FCFs	0.6721	0.1621	0.1168	0.0353	0.0104
	$T_{v'v''}$	24563	25124	25574	26117	26663
1	$A_{v'v''}$	8.3042	1.0778	6.4040	6.0378	3.6396
	FCFs	0.2414	0.0431	0.2541	0.2437	0.1392
	$T_{v'v''}$	23544	24105	24555	25099	25644
2	$A_{v'v''}$	1.7149	3.8461	2.9542	0.2172	3.9604
	FCFs	0.0568	0.1751	0.1329	0.0099	0.1709
	$T_{v'v''}$	22535	23096	23546	24090	24635
3	$A_{v'v''}$	0.4318	3.4832	0.0314	2.8807	1.6088
	FCFs	0.0164	0.1810	0.0016	0.1493	0.0786
	$T_{v'v''}$	21536	22097	22547	23090	23636
4	$A_{v'v''}$	0.1672	2.5624	0.5235	1.5826	0.1955
	FCFs	0.0073	0.1528	0.0307	0.0935	0.0109
	$T_{v'v''}$	20547	21108	21557	22101	22647
5	$A_{v'v''}$	0.0734	1.7560	1.2566	0.1693	1.2970
	FCFs	0.0037	0.1207	0.0847	0.0115	0.0823
	$T_{v'v''}$	19567	20128	20578	21121	21667

coefficient ($A_{v'} = \sum_{v''} A_{v'v''}$). On the basis of Einstein coefficient $A_{v'v''}$ given in Tables 6–9, the radiative lifetimes of the five lowest vibrational states of the $A^1\Pi$, $A'^1\Sigma^+$, $a^3\Pi_{0+}$, and $a^3\Pi_1$ states were computed, as listed in Table 10. The evaluated radiative lifetimes of $A^1\Pi$ and $A'^1\Sigma^+$ are on the order of 100 and 10 ns, respectively, whereas those of $a^3\Pi_{0+}$ and $a^3\Pi_1$ are on the order of 1 ms and 0.1 ms, respectively. It can be found from Tables 9 and 10 that the transition energies and FCFs of $a^3\Pi_{0+}$ and $a^3\Pi_1$ are similar on the whole; hence, the larger lifetime of $a^3\Pi_{0+}$ relative to that of $a^3\Pi_1$ is caused by the smaller TDM of $a^3\Pi_{0+}$ near the equilibrium bond length.

CONCLUSIONS

In summary, we calculated the PECs of 18 low-lying Λ–S states of CSe molecule by employing the MRCI+Q approach with the all-electronic entirely uncontracted aug-cc-pwCV5Z basis set. The scalar relativity effect was also included by utilizing the second-order one-electron Douglas–Kroll–Hess method. For better accuracy, the PECs of low-lying Ω states of CSe were computed utilizing the state-interacting method with the full Breit-Pauli Hamiltonian.

Table 10. Radiative Lifetimes (ns) of the Low-Lying Vibrational Levels of $A'^1\Sigma^+(A')$, $A^1\Pi(A)$, $a^3\Pi_1(a1)$, and $a^3\Pi_{0+}(a_{0+})$

	radiative lifetimes			
v'	$\tau_{A'-X}$	τ_{A-X}	τ_{a1-X}	τ_{a0+-X}
0	46	218	0.27×10^6	2.54×10^6
1	49	227	0.52×10^6	2.00×10^6
2	53	238	0.54×10^6	1.47×10^6
3	58	258	0.64×10^6	1.46×10^6
4	64	271	0.67×10^6	1.12×10^6

On the basis of the calculated PECs of Λ–S and Ω states, the spectroscopic parameters of bound electronic states were obtained, which are consistent with previously available experimental and theoretical results. A strong state interaction is expected due to the large state density in the investigated energy region. The SOC of the $A^1\Pi$ and $a^3\Pi$ states with other electronic states is studied in this work. The PECs of the $A^1\Pi$ and $a^3\Pi$ states cross with that of the $1^1\Sigma^-$, $1^1\Delta$, $a'^3\Sigma^+$, $d^3\Delta$, and $e^3\Sigma$ states at the bond length region 1.55–2.15 Å. Around the crossing points, our calculated values of nonvanishing spin–orbit matrix elements including $A^1\Pi$ and $a^3\Pi$ states are computed in the range 201.5–275.7 cm^{-1}, which are large enough to perturb corresponding vibrational levels of $A^1\Pi$ and $a^3\Pi$ states. With the aid of the calculated spin–orbit matrix elements, the Λ–S compositions of Ω states at different bond lengths and the PECs of the Ω-states, we analyze the spin–orbit perturbations to the $A^1\Pi$ and $a^3\Pi$ states, illuminating the avoided crossing phenomenon in the PECs of Ω states caused by the SOC effect. The TDMs of two spin-allowed $A^1\Pi$–$X^1\Sigma^+$ and $A'^1\Sigma^+$–$X^1\Sigma^+$ transitions, and two spin-forbidden $a^3\Pi_{0+}$–$X0^+$ and $a^3\Pi_1$–$X0^+$ transitions, were also evaluated in the SOC calculations. The lifetimes of low-lying vibrational states of $A^1\Pi$, $A'^1\Sigma^+$, $a^3\Pi_{0+}$, and $a^3\Pi_1$ were obtained from TDMs, FCFs, and transition energies. Our investigation suggests that the SOC effect plays a significant role in the spectroscopic properties of CSe molecule. The present theoretical study could support further experimental studies on the structure and spectroscopic properties of the low-lying electronic states of CSe molecule.

ASSOCIATED CONTENT

Supporting Information

Data of potential energy curves (PECs) of the Λ–S electronic states in Figure 1 are summarized in Table S1. Data of PECs of the low-lying Ω electronic states in Figure 5 are summarized in Table S2. Composition of Ω states of CSe at different bond lengths are provided in Table S3. This material is available free of charge via the Internet at http://pubs.acs.org.

AUTHOR INFORMATION

Corresponding Authors

*H.X.: tel, 86-431-85168817; fax, 86-431-85168816; email, xuhf@jlu.edu.cn.

*B.Y.: tel, 86-431-85168817; fax, 86-431-85168816; email, yanbing@jlu.edu.cn.

Notes

The authors declare no competing financial interest.

■ ACKNOWLEDGMENTS

This work was supported by National Basic Research Program of China (973 Program) (2013CB922200) and National Natural Science Foundation of China (11034003, 11074095, and 11274140). R.L. also acknowledges the support by the Educational Science Research Foundation of Qiqihar University (2012050) and Scientific Research Fund of the Heilongjiang Provincial Education Department (12531751). We acknowledge the High Performance Computing Center (HPCC) of Jilin University for supercomputer time.

■ REFERENCES

(1) Wittig, C. Carbon Monoxide Chemical Laser from the Reaction O + CSe → CO† + Se. *Appl. Phys. Lett.* **1972**, *21*, 536−538.
(2) Rosenwaks, S.; Smith, I. W. M. Laser Emission from CO Formed in the Flash-Initiated Reactions of O(^{3}P) Atoms with CS and CSe. *J. Chem. Soc., Faraday Trans. 2* **1973**, *69*, 1416−1424.
(3) Lin, M. C.; Umstead, M. E.; Djeu, N. Chemical Lasers. *Annu. Rev. Phys. Chem.* **1983**, *34*, 557−591.
(4) Barrow, R. F. A Reinvestigation of the Ultra-Violet Band System of Carbon Monoselenide. *Proc. Phys. Soc.* **1939**, *51*, 989−991.
(5) Laird, R. K.; Barrow, R. F. The Ultra-Violet Band Spectrum of Carbon Monoselenide. *Proc. Phys. Soc. Sect. A* **1953**, *66*, 836−839.
(6) Howell, H. G. On the Spectra of CS and CSe. *Proc. Phys. Soc.* **1947**, *59*, 107−111.
(7) Lebreton, J.; Bosser, G.; Marsigny, L. New Emission Spectrum of Carbon Monoselenide. *J. Phys. B: At. Mol. Phys.* **1973**, *6*, L226−L227.
(8) Bosser, G.; Lebreton, J. Rotational Analysis of the $a^3\Pi_{1,0+}$ to $X^1\Sigma^+$ System of Carbon Monoselenide. *J. Phys. B: At. Mol. Phys.* **1981**, *14*, 1445−1448.
(9) Martin, J. M. L.; Sundermann, A. Correlation Consistent Valence Basis Sets for Use with the Stuttgart−Dresden−Bonn Relativistic Effective Core Potentials: The Atoms Ga−Kr and In−Xe. *J. Chem. Phys.* **2001**, *114*, 3408−3420.
(10) Kalcher, J. Trends in Ground and Excited State Electron Affinities of Group 14, 15, and 16 Mixed Diatomic Anions: a Computational Study. *Phys. Chem. Chem. Phys.* **2002**, *4*, 3311−3317.
(11) Menconi, G.; Tozer, D. J. Diatomic Bond Lengths and Vibrational Frequencies: Assessment of Recently Developed Exchange-Correlation Functionals. *Chem. Phys. Lett.* **2002**, *360*, 38−46.
(12) Liu, H.; Shi, D. H.; Sun, J. F.; Zhu, Z. L. Spectroscopic Parameters and Molecular Constants of CSe($X^1\Sigma^+$) Radical. *Acta Phys. Sin.* **2011**, *60*, 063101.
(13) Li, R.; Wei, C.; Sun, Q.; Sun, E.; Xu, H.; Yan, B. Ab Initio MRCI +Q Study on Low-Lying States of CS Including Spin-Orbit Coupling. *J. Phys. Chem. A* **2013**, *117*, 2373−2382.
(14) Minaev, B.; Plachkevytch, O.; Ågren, H. Multiconfiguration Response Calculations on the Cameron Bands of the CO Molecule. *J. Chem. Soc., Faraday Trans.* **1995**, *91*, 1729−1733.
(15) Werner, H.-J.; Knowles, P. J.; Lindh, R.; Manby, F. R.; Schütz, M.; Celani, P.; Korona, T.; Mitrushenkov, A.; Rauhut, G.; Adler, T. B.; et al. *MOLPRO*, a package of ab initio programs, 2010.
(16) Peterson, K. A.; Dunning, T. H. Accurate Correlation Consistent Basis Sets for Molecular Core−Valence Correlation Effects: The Second Row Atoms Al−Ar, and the First Row Atoms B−Ne Revisited. *J. Chem. Phys.* **2002**, *117*, 10548−10560.
(17) DeYonker, N. J.; Peterson, K. A.; Wilson, A. K. Systematically Convergent Correlation Consistent Basis Sets for Molecular Core−Valence Correlation Effects: The Third-Row Atoms Gallium through Krypton. *J. Phys. Chem. A* **2007**, *111*, 11383−11393.
(18) Werner, H. -J.; Knowles, P. J. A Second Order Multiconfiguration SCF Procedure with Optimum Convergence. *J. Chem. Phys.* **1985**, *82*, 5053−5063.
(19) Knowles, P. J.; Werner, H.-J. An Efficient Second-Order MCSCF Method for Long Configuration Expansions. *Chem. Phys. Lett.* **1985**, *115*, 259−267.
(20) Werner, H.-J.; Knowles, P. J. An Efficient Internally Contracted Multiconfiguration-Reference Configuration Interaction Method. *J. Chem. Phys.* **1988**, *89*, 5803−5814.
(21) Knowles, P. J.; Werner, H.-J. An Efficient Method for the Evaluation of Coupling Coefficients in Configuration Interaction Calculations. *Chem. Phys. Lett.* **1988**, *145*, 514−522.
(22) Langhoff, S. R.; Davidson, E. R. Configuration Interaction Calculations on the Nitrogen Molecule. *Int. J. Quantum Chem.* **1974**, *8*, 61−72.
(23) Douglas, M.; Kroll, N. M. Quantum Electrodynamical Corrections to the Fine Structure of Helium. *Ann. Phys.* **1974**, *82*, 89−155.
(24) Hess, B. A. Relativistic Electronic-Structure Calculations Employing a Two-Component No-Pair Formalism with External-Field Projection Operators. *Phys. Rev. A* **1986**, *33*, 3742−3748.
(25) Berning, A.; Schweizer, M.; Werner, H.-J.; Knowles, P. J.; Palmieri, P. Spin-Orbit Matrix Elements for Internally Contracted Multireference Configuration Interaction Wavefunctions. *Mol. Phys.* **2000**, *98*, 1823−1833.
(26) LeRoy, R. J. *LEVEL7.7: A computer program for solving the radial Schrödinger equation for bound and quasibound levels*; Chemical Physics Research Report CP-661; University of Waterloo: Ontario, Canada, 2005.
(27) Stringat, R.; Bacci, J.-P.; Pischedda, M.-H. Rotational Analysis of the $^1\Pi$−$X^1\Sigma^+$ System of $C^{80}Se$. *Can. J. Phys.* **1974**, *52*, 813−820.
(28) Cossart, D.; Bergeman, T. Offdiagonal Spin−Orbit and Apparent Spin−Spin Parameters in Carbon Monosulfide. *J. Chem. Phys.* **1976**, *65*, 5462−5468.
(29) Moore, C. E. *Atomic Energy Levels*; National Bureau of Standards: Washington, DC, 1971.